

Supplementary material

Structural and Optical Characterization of ZnO-ZrO₂ Nanocomposites for Photocatalytic Degradation and Mineralization of Phenol

M. Uribe¹, M.A Alvarez Lemus^{1*}, M.C. Hidalgo², R. López¹, P. Quintana³, S. Oros⁴,
S. Uribe^{1a}, J. Acosta¹

¹Nanotechnology for Biomedicine and Environmental Applications, ^{1a}CONACYT-Research Fellow, Academic Division of Engineering and Architecture, Juárez Autonomous University of Tabasco, Carr. Cunduacán Jalpa de Méndez Km 1, Col. La Esmeralda, CP 86690, Cunduacan, Tabasco, México.

² Instituto de Ciencia de Materiales de Sevilla (ICMS), Consejo Superior de Investigaciones Científicas (CSIC)-Universidad de Sevilla, Américo Vespucio 49, 41092 Sevilla, España

³ Departamento de Física Aplicada, CINVESTAV Unidad Mérida, AP. 73 Cordemex, 97310, Mérida Yucatán, México

⁴ CONACYT-Research Fellow-Department of Chemistry, ECOCATAL group, Autonomous Metropolitan University – Iztapalapa, Av. San Rafael Atlixco No. 186, Col. Vicentina, Iztapalapa, 09340, México

*Corresponding autor: mayra.alvarez@ujat.mx

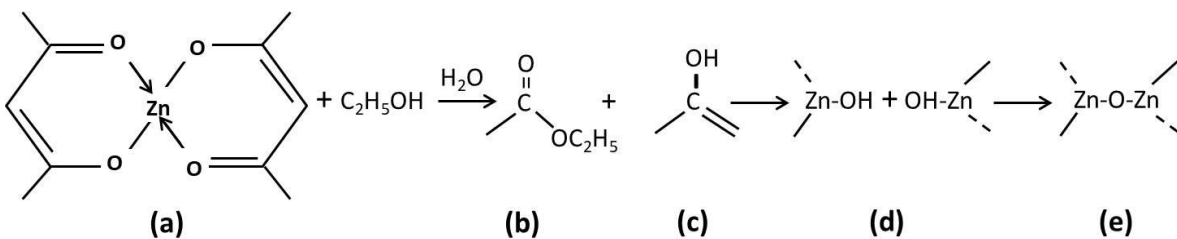


Figure S1. Proposed reactions of ZnO formation. The mechanism shows a nucleophilic attack of ethanol on one of the carbonyl groups of the acetylacetone ligand (a), hydrolysis leading to the formation of ethyl acetate (b) and acetone in its enolate form (c) from the nucleophilic attack of the water molecule present in the precursor hydrate species. This results in the formation of Zn–OH species (d), which represent the monomeric units for the nucleation of ZnO nanocrystals, which proceeds through the formation of Zn–O–Zn bonds (e) via the condensation reaction [1] [2].

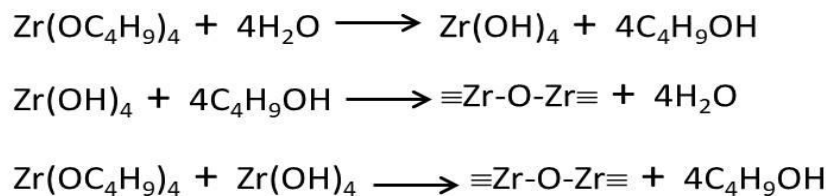


Figure S2. Proposed reactions for the formation of ZrO₂ nanoparticles from Zirconium(IV) butoxide by sol-gel process [3].

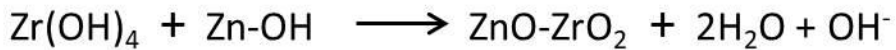


Figure S3. Proposed mechanism for the formation of ZnO-ZrO₂ nanocomposites by sol-gel.

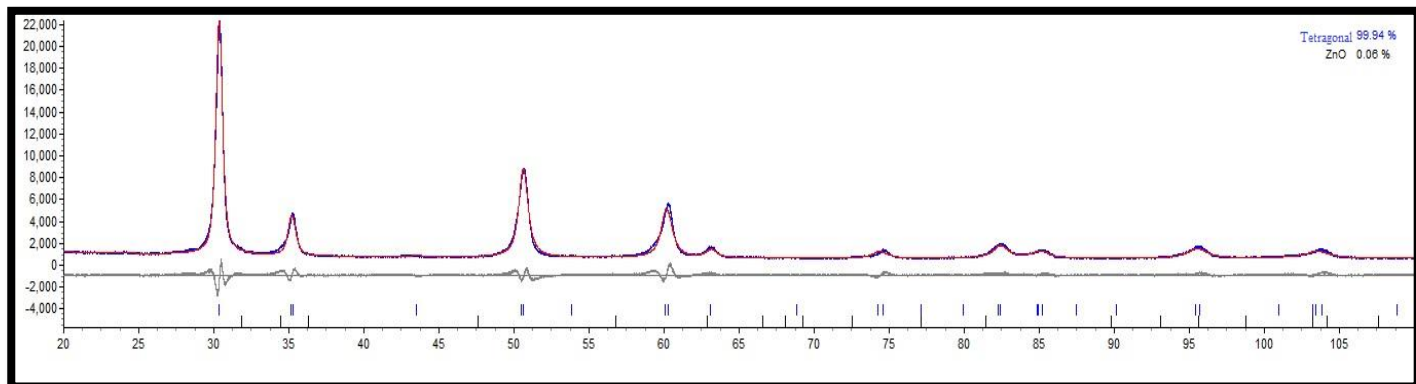


Figure S4. Graphic view of Rietveld refinement of 13ZnO-ZrO₂. Gray line represents the difference between calculated and experimental pattern, red line is the calculated pattern whereas blue line experimental pattern. The sample presents tetragonal phase of ZrO₂ and wurzite of ZnO, whereas cubic and monoclinic phase of ZrO₂ was not detected. No solid solution was formed.

Refinement data:

R _{exp} : 2.86	R _{wp} : 7.75	R _p : 6.06	GOF : 2.71
R _{exp`} : 4.75	R _{wp`} : 12.85	R _{p`} : 11.14	DW : 0.27

Table S1. Lattice parameters of the composites obtained from Rietveld refinement.

Sample	Lattice parameters	Rwp
13ZnO-ZrO ₂	ZrO ₂ -Tetragonal phase: a (Å)=3.6109 c (Å)=5.0845 ZnO-Wurzite structure: a (Å)= 3.2419 c (Å)= 5.2070	Rexp: 2.86 Rwp: 7.75 Rp: 6.06 GOF: 2.71 Rexp`: 4.75 Rwp: 12.85 Rp: 11.14 DW: 0.27

Table S2. Band gap values of ZnO, ZrO₂ and ZnO-ZrO₂ composites. A direct transition for ZnO and indirect transition for ZrO₂ and ZnO-ZrO₂ were used, because of the highly accurate results obtained.

Sample	Eg (eV)	R ²	Eg (eV)	R ²

ZnO	3.26	0.99257	-	-
ZrO ₂	4.53	0.99907	5.06	0.99703
13ZnO-ZrO ₂	4.73	0.99953	3.07	0.98750
25ZnO-ZrO ₂	4.35	0.99825	3.10	0.97904
50ZnO-ZrO ₂	3.76	0.99678	3.15	0.99103
75ZnO-ZrO ₂	4.16	0.99914	3.16	0.97762

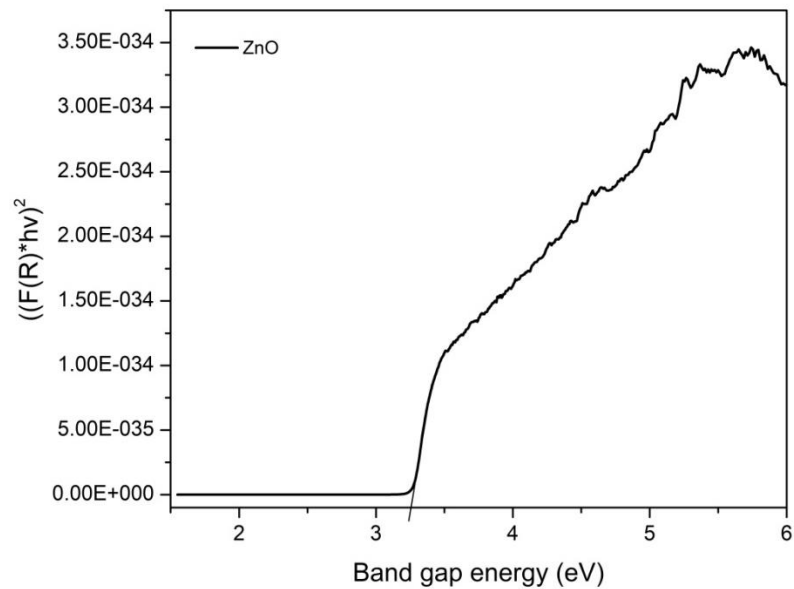


Figure S5. Plot of Kubelka-Munk function vs energy to obtain the band gap enegy of ZnO.

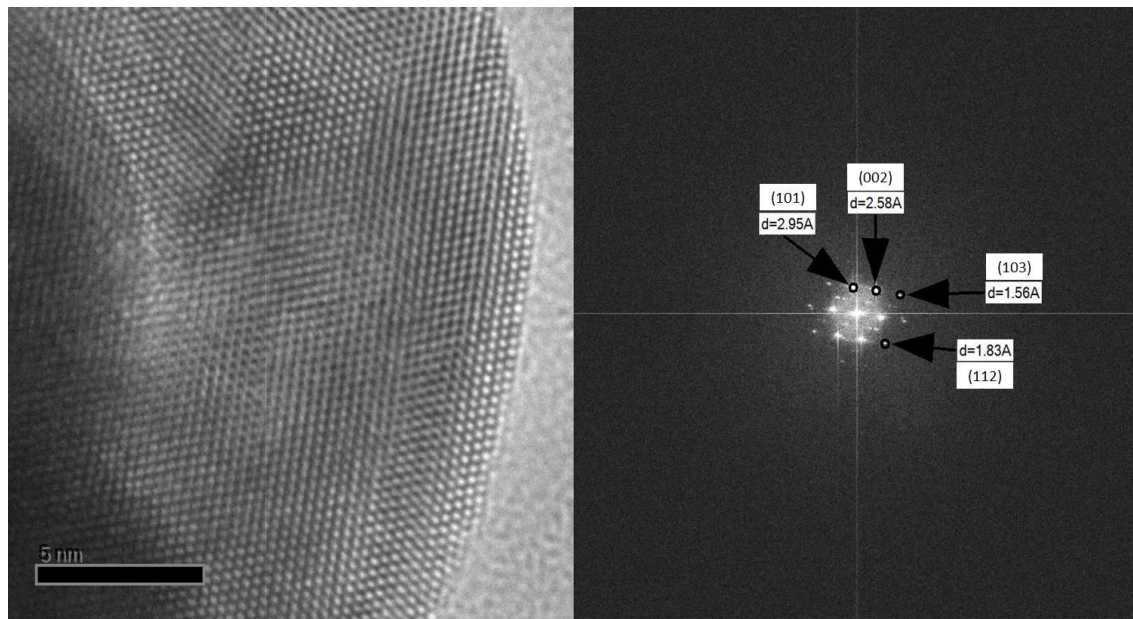


Figure S 6. TEM micrograph of tetragonal phase of ZrO_2 in the 13ZnO-ZrO₂ sample.

REFERENCES

- [1] B. Ludi y M. Niederberger, "Zinc oxide nanoparticles: chemical mechanisms and classical and non-classical crystallization", *Dalton Transactions*, vol. 42, núm. 35, pp. 12554–12568, 2013.
- [2] G. Ambrožič, S. D. Škapin, M. Žigon, y Z. C. Orel, "The synthesis of zinc oxide nanoparticles from zinc acetylacetone hydrate and 1-butanol or isobutanol", *Journal of Colloid and Interface Science*, vol. 346, núm. 2, pp. 317–323, 2010.
- [3] U. K. H. Bangi, C.-S. Park, S. Baek, y H.-H. Park, "Sol-gel synthesis of high surface area nanostructured zirconia powder by surface chemical modification", *Powder Technology*, vol. 239, pp. 314–318, 2013.